



First-principles study of structural, electronic and optical properties of AgSbO_3 and $\text{AgSb}_{0.78}\text{Se}_{0.22}\text{O}_3$ photocatalyst

Mohammad Jahidul Islam¹ · Ajoy Kumer² Received: 19 November 2019 / Accepted: 15 January 2020 / Published online: 22 January 2020
© Springer Nature Switzerland AG 2020

Abstract

The electronic band structures, density of state, partial density of state, optical properties, and photocatalytic activities under visible light were investigated using first principle method for AgSbO_3 crystal and Se doped. Using generalized gradient approximation based on the Perdew–Burke–Ernzerhof (PBE0), the band gap was found 0.301 eV. To recognize the character of photocatalyst activity, the optical properties were calculated. On the other hand, it was improved by using the doped of 0.22 portions Se metalloid in the crystals, its band gap was 0.16 eV whatever photocatalytic activity was increased. The second point is the optical properties as well as absorption, reflection, refractive index, conductivity, dielectric function, and loss function. After doping by Se with AgSbO_3 , the optical properties are regularly changed and increased the photocatalytic effect due to the hybridization of 4s, 3d and 4p orbitals of Se with 5s, 4d and 5p orbitals of Sb.

Keywords AgSbO_3 · Se-doped · Band gap · Density of state · Optical properties

1 Introduction

The semiconductor based photocatalyst has attracted great interest in the last two decades to degrade organic pollutants especially dye molecules from eliminating textile industries by means of low cost and environmentally benign chemicals [1]. It was reported that TiO_2 , WO_3 , CdS, ZnSe, GaAs, GaP, etc. semiconductors were used as a photocatalyst, in particular, TiO_2 has been investigated due to its high chemical stability, photocatalytic activity, and non-toxicity [2]. The vital industries in Bangladesh are textile, and readymade garments and the secondary growing areas are fertilizer industries, agricultural industries, food and beverage industries, etc. [3, 4]. The most important key point of the gross domestic product (GDP) and economical scale stands on the textile and readymade garment industries for the last 2 decades where more than 20 million Bangladeshi people are connected for their life hood [5, 6]. There are produced million tons of waste from

dye, operative process, and textile chemicals. But the traditional degradation process or ETP operation is related to highly expensive, for instance, US\$ 4–5 is need to treat for 10 m³ waste water in ETP [7]. The alternative environmental benign process is the photodegradation of textile dyes and chemicals [8]. In the photocatalysis process, the main function of photocatalyst is to absorb photons from artificial or natural lights and generates excited electron–hole pairs [9]. After separating with each other, the electrons and holes travel to the photocatalyst solution interface and activate the hydrogen evolution reaction and evolution of oxygen under visible light or sunlight [10]. In this case, to develop a new material for acting photocatalyst is required the formation of a new valence band or conduction band state above the 2p orbital or metal 3d orbital through orbital hybridization [11].

Developing the concept of the photocatalyst in computationally is linked to the band gap and density of state which is also related conduction band and valence

✉ Ajoy Kumer, kumarajoy.cu@gmail.com | ¹Department of Physics, European University of Bangladesh, Dhaka 1216, Bangladesh. ²Department of Chemistry, European University of Bangladesh, Dhaka 1216, Bangladesh.



band. It was established that a band gap larger than 1.23 eV, the photocatalyst must also have its conduction band higher than the $\text{H}_2/\text{H}_2\text{O}$ redox state in solution and have its valence band lower than the $\text{O}_2/\text{H}_2\text{O}$ redox level in solution [12, 13]. Finally it can be said that for becoming photocatalytic behavior, generally the materials must have less the 1.23 eV energy gap.

On the basis of semiconductor photocatalyst, the most AgSbO_3 is targeted molecule to develop as photocatalyst in views of computational concepts because it was estimated the photocatalytic activity [14]. As AgSbO_3 is considered as a novel visible light responsive photocatalyst, calculation the band structure, the valence band is made of hybridized Ag 4*d* and O 2*p* orbital and the lower of the conduction band mainly consists of the 5*s* for Ag and the 5*s*, 5*p* for Sb orbital [15]. It was reported that the AgSbO_3 shows a higher O_2 evolution activity than WO_3 or another photocatalyst. The second key point the hybridized 4*s* and 5*p* orbital of Se metalloid which make numerous effects of both of conduction band and valence band as doping with AgSbO_3 [16]. To explain the optical activity of AgSbO_3 , the refractive index, absorption, dielectric function, conductivity, and loss function were calculated. After Se-doped with AgSbO_3 crystal molecules, the band gap and density of state are compared with the undoped crystals. As Se metalloid increased photocatalytic activity under visible light of TiO_2 , it was interesting to choose as a doping metalloid in AgSbO_3 crystal in this research [17].

2 Computational methods

To calculate the energy gap and density of state, the method of GGA with PBE0 was used in the option of CASTEP code from material studio [18]. In this condition, the cut off was 523, and k point was $2 \times 2 \times 3$ with norm-conserving pseudopotentials by which the band gap and density of state were calculated. The second steps to calculate the optical properties, this similar way were used for calculation of refractive index, reflectivity, absorption, conductivity, and loss function. Geometric optimization was achieved and the convergence criterion for the force between atoms was 3×10^{-6} eV/Å, the maximum displacement was 1×10^{-3} Å, and the total energy and the maximal stress were 1×10^{-5} eV/atom and 5×10^{-2} GPa, respectively. Se metalloid was doped replacing Sb atoms in the crystals in AgSbO_3 by 0.22 portions or 22% percentage. One of the key features of this work was minimum portion doped by Se metalloid into the crystal structure. The crystal structure was in a symmetry pattern that is why the minimum portion of doping by 22% was optimized.

3 Results and discussion

3.1 Optimized structure

The lattice parameters value of $a = 8.166$ Å, $b = c = 8.317$ Å and bond angles them as $\alpha = 110.252^\circ$, $\beta = \gamma = 109.428^\circ$ are listed for monoclinic AgSbO_3 respectively [15]. The monoclinic AgSbO_3 crystal and the space group is Hermann Mauguin, C2, monoclinic crystal system, point group 2, hall C 2y, density 6.42 g/cm³ shown in Fig. 1a, and the Se doped optimized structure is accounted in Fig. 1b.

3.2 Band structure

The band structures of AgSbO_3 with PBE are determined and the Fermi is set as zero. The minimum different of conduction bands (CB) and valence bands are obtained at G symmetry point illustrated in Fig. 2a, b. It indicates that AgSbO_3 is a direct band gap semiconductor. The direct gap from G (CB) to G (VB) is calculated to be 0.301 eV. The GGA method (PBE0) gives a much more credible band gap of 0.301 eV, which agrees well with the experimental value of 0.289 eV [19]. From this Fig. 2a, it can be said that the lower parts of the conduction band are well dispersive in the G symmetry point while the symmetry point at L, M, A, Z, and V are comparatively smaller splitting but the upper part is not dispersive as like the lower portions. In general, a lower carrier effective mass corresponds to higher carrier mobility. So the photogenerated electrons in the conduction band can transfer more rapidly to the surface of AgSbO_3 to participate in the photocatalytic reaction or photocatalytic solution. The second key factor is doping by Se metalloid with 0.22 portions or 22% percentage of Se using regenerating super cell in materials studio, the band gap was calculated with same methods and obtained data shown in Fig. 2b. The upper levels of valence band were obtained at point M and the lower point of conduction band was found at symmetry point G. The band gap is located between the different M symmetry and G symmetry points where have the value 0.16 eV. Due to adding Se as doping, there is a change in the upper level of conduction band which is dispersed at M and G symmetry point, and the upper band is also decreased at A and Z points while in case of valence band, there are not any changed compared to undoped.

3.3 Density of state

The density of the state indicates the nature of electronic band structures and the splitting of orbitals. The total density of states (TDOS) of Ag, Sb, and O elements for

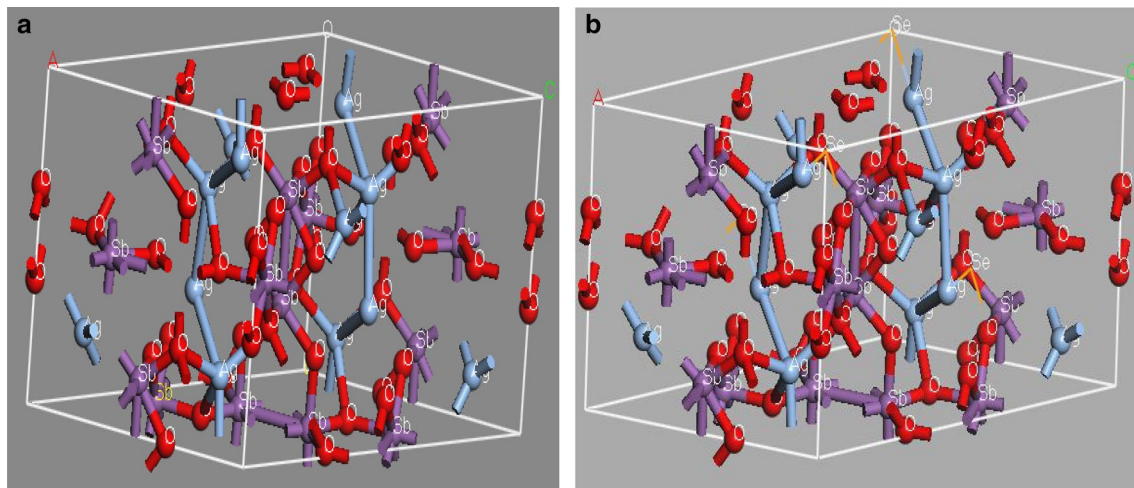


Fig. 1 Optimized structure for **a** undoped AgSbO_3 , **b** Se doped AgSbO_3

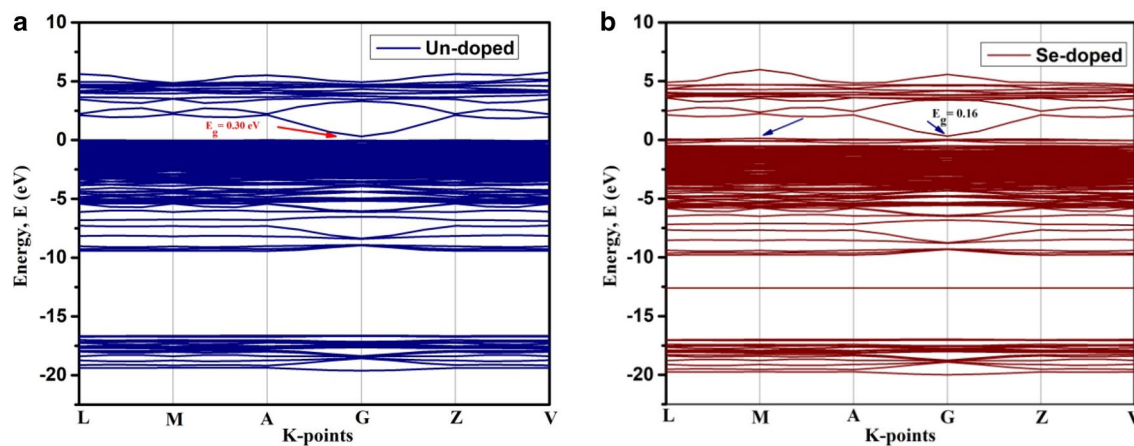
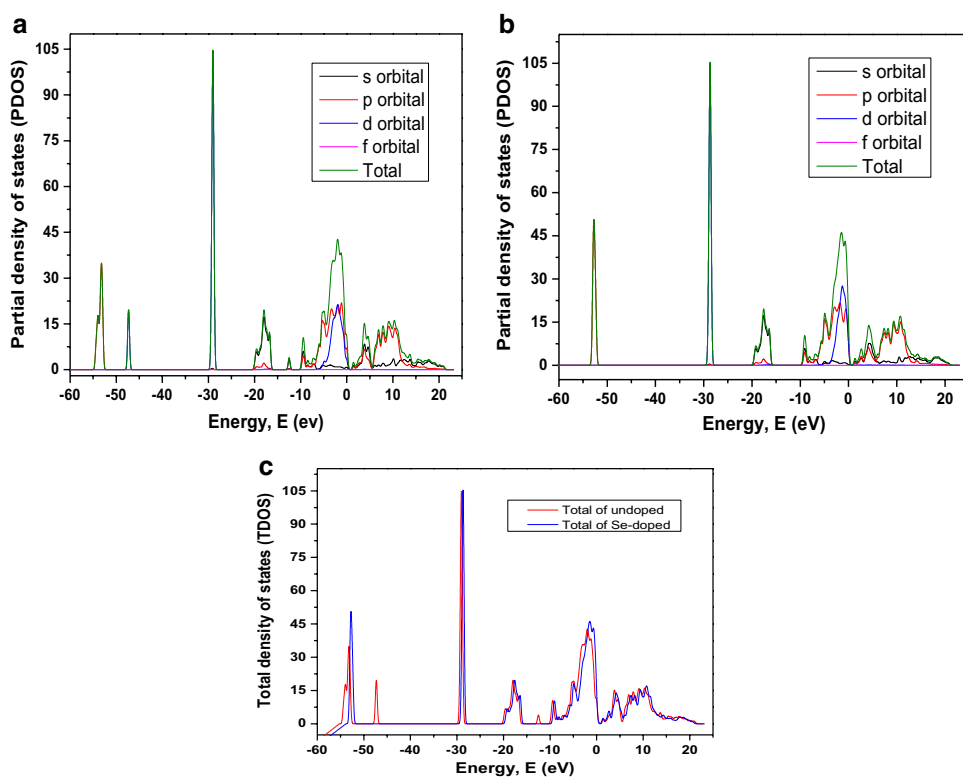


Fig. 2 Band gap of **a** undoped, **b** doped by Se 0.22 portions

AgSbO_3 crystal was calculated by PBE0 with GGA. From Fig. 3, it was found that the valence bands are mainly occupied by $2p$ state for O, $4d$ and $5s$ state for Ag and $4d$ and $5p$ state for Sb elements. Meanwhile, more the Fermi level, the conduction bands are composed of Ag in $5s$, $4d$ orbitals whereas the conduction band of Sb also consists of $5p$, $5d$ orbitals, and $2s$ and $2p$ orbitals for O atom. As shown in Fig. 3a–c, the bands just below the Fermi level and above the Fermi level in the range from -7 to 0 eV, -20 to 20 eV, and -30 to 22 eV are contributed mainly by the d , p , and s orbital for AgSbO_3 respectively. This character is beneficial for the transfer of photogenerated electrons in the MCB. Thus the photogenerated electrons in the MCB of AgSbO_3 can be rapidly transferred to the surface to participate in the reaction. After that, from Fig. 3b, when the Se metalloid was doped with AgSbO_3 ,

there was obtained another density of state in energy from -55 to 20 eV that is found due to the $4s$ $4p$ and $3d$ of Se with Sb due to hybridization. The $3d$ orbital of Se is more localized than $4s$ and $4p$, moreover comparing the Fig. 3a, b, the d orbital of doped is more localized, for instance undoped is about 20 while doped is about 30. From Fig. 3c, it is accounted for total density of states in Se doped of AgSbO_3 is more delocalized than undoped AgSbO_3 almost each photon energy. For this reason, the photogenerated electrons of $\text{AgSb}_{0.78}\text{Se}_{0.22}\text{O}_3$ can easily transferred than AgSbO_3 which is mentioned that the dye degradation by $\text{AgSb}_{0.78}\text{Se}_{0.22}\text{O}_3$ is enhanced than AgSbO_3 . This gives a further detailed explanation of the high photocatalytic performance of the AgSbO_3 doped Se metalloid.

Fig. 3 Density of states **a** of undoped, **b** for Se doped. **c** Total Density of States of undoped and doped



3.4 Optical properties

The photocatalytic nature of photocatalyst depends on the light absorption, charge transportation and a number of active sites that are related to band gap magnitude and electrons or holes mobilities in regarding conductivity, reflectivity and refractive index. The second required point as the number of active sites including a large surface area of the molecule is favored because it provides a greater number of surface active sites for the adsorption of organic molecules, thus increasing their decomposition/oxidation.

3.4.1 Optical reflectivity

To explain the photocatalytic activity, the optical reflectivity of crystal plays an important role in how much light is reflected from the material in relation to an amount of light incident on the photocatalytic solution of pollutants or a rough surface and scattering volume is diffused. The second key point is related to absorption. The lower reflectivity indicated the higher UV or visible light absorption. From Fig. 4, the reflectivity of Se doped has slightly lower than undoped of AgSbO₃, standing for the increasing the photocatalytic effect on pollutants.

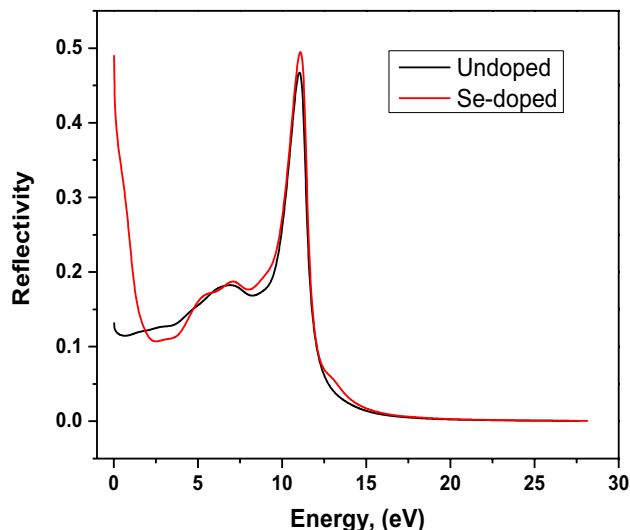


Fig. 4 Reflectivity for undoped and Se doped

3.4.2 Absorption

Optical adsorption is optimized by the function of polycrystalline where the electric field over all directions. In order to better distinguish the absorption peaks, small smearing of 0.1 eV is applied. As shown in Fig. 5, this peak is contributed by the photo transition energies from the MVB to the MCB under visible light irradiation, indicating

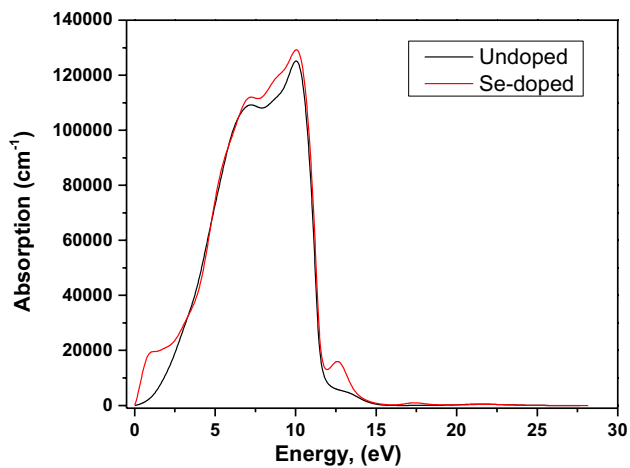


Fig. 5 Absorption for undoped and Se doped

that AgSbO_3 is a visible-light-response photocatalyst whereas the Se doped crystal shows on more peak than undoped and indicating higher absorption.

As absorption is directly related to electromagnetic radiation, belongs to the photon energy. In case of photocatalytic effect greater absorption indicates the higher degradation of chemicals or pollutants. From Fig. 5, in lower frequency the absorption both of undoped and doped crystal is almost zero. In both doped and undoped show the regular change before 15 eV photon energy, while the Se doped AgSbO_3 illustrates the higher absorption than undoped AgSbO_3 . Thus due to Se doping in AgSbO_3 absorption was increased as well as photocatalytic activity was increased.

3.4.3 Refractive index

The refractive index is the most important parameter for measuring light absorption throughout the photocatalytic effect on degradation. A greater refractive index indicates the greater denser medium. From the Fig. 6, it could be explained that the refractive index initially of the undoped AgSbO_3 shows the near 2 at frequency 12 eV whereas the Se doped was 4.5 but after increasing frequency, Se doped AgSbO_3 rapidly decreases in the minimum range at 0.4 for frequency about 10 eV. Finally, both crystals can show a similar refractive index after frequency 15 having refractive index 1. From the comparison of real part of reflective index for $\text{AgSb}_{0.78}\text{Se}_{0.22}\text{O}_3$, it is slightly higher than AgSbO_3 . As result it is chemically more stable.

3.4.4 Dielectric function

Due to having the optical adsorption property of semiconductors, shows a large affinity to photocatalytic

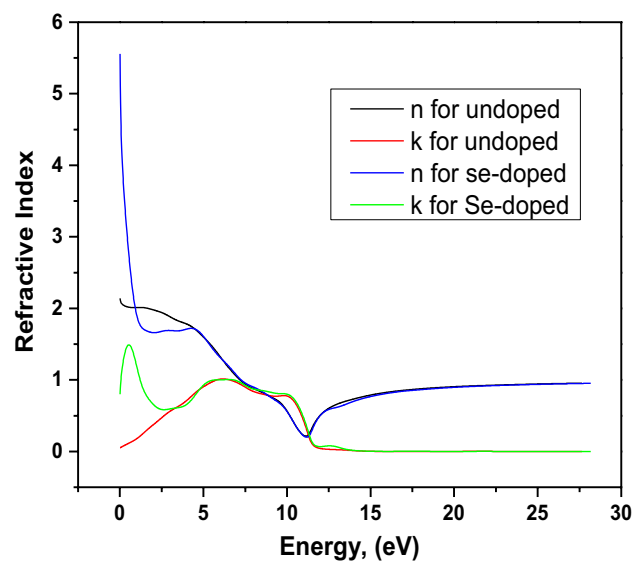


Fig. 6 Refractive index for undoped and Se doped

effect and dielectric function is a very necessary tool to investigate their optical properties which are related to adsorption properties as the following equation for solid.

$$\varepsilon = \varepsilon_1(\omega) + i\varepsilon_2(\omega)$$

where $\varepsilon_1(\omega)$ and $\varepsilon_2(\omega)$ are denoted the real part and the imaginary part of the dielectric function, respectively. The dielectric function has a relationship with space or frequency of materials. The dielectric function is physically equivalent to the permittivity or absolute permittivity. From this Fig. 7, it is found that initially, those fluctuated

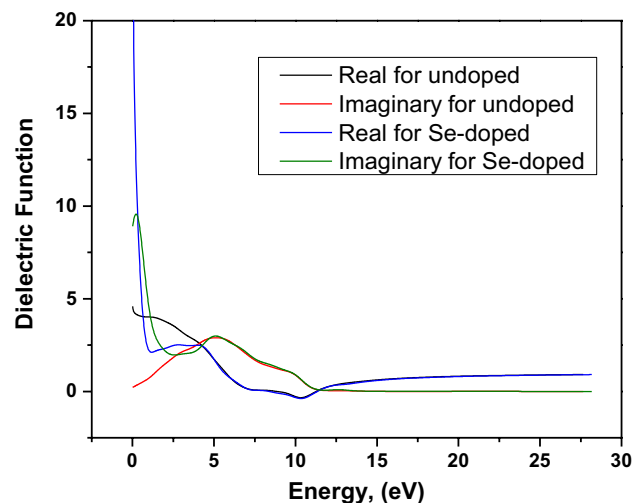


Fig. 7 Dielectric function for undoped and Se doped

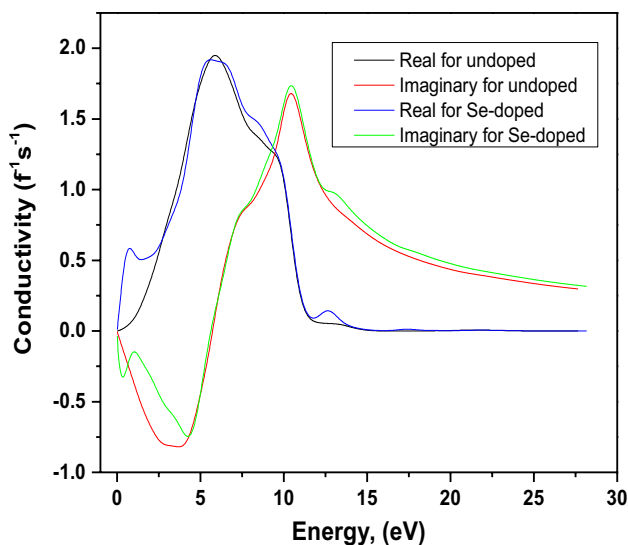


Fig. 8 Conductivity for undoped and Se doped

slightly before frequency 15 after that those are similar patterns of the dielectric function.

3.4.5 Conductivity

The conductivity of the semiconductor on basis of the energy band and orbitals electrons is linked with the discrete space of electrons in orbit. This is also produced due to the presence of holes and free electrons in the crystal molecules. The energy gap between MCB and MVB for photocatalyst is less than 1.8 eV. From Fig. 8, the conductivity between MCB and MVB of undoped AgSbO_3 is about 1.9 eV which is almost overlapping for good photocatalyst whereas the conductivity for Se doped AgSbO_3 is around 1.8 eV. It is concluded that after 0.22 portions of doping by Se metalloids with AgSbO_3 , the conductivity is poorly increased for both of real and imaginary part.

3.4.6 Loss function

There are two regions for electronic energy loss function such as high energy region or low energy region for optical properties. The first region is the high loss energy region with the change of frequency or spectra after the ionization edge which can say the oxidation state of d orbital splitting for metals of center atom in complex compounds, having the range the more 10 eV. The other is the low energy loss function, including the energy less than 1, which can provide information about the composition and electronic structure. The energy loss function for optical properties is linked to the dielectric constant of the materials within the range of validity of the dielectric theory. From Fig. 9, it could be said that the loss energy

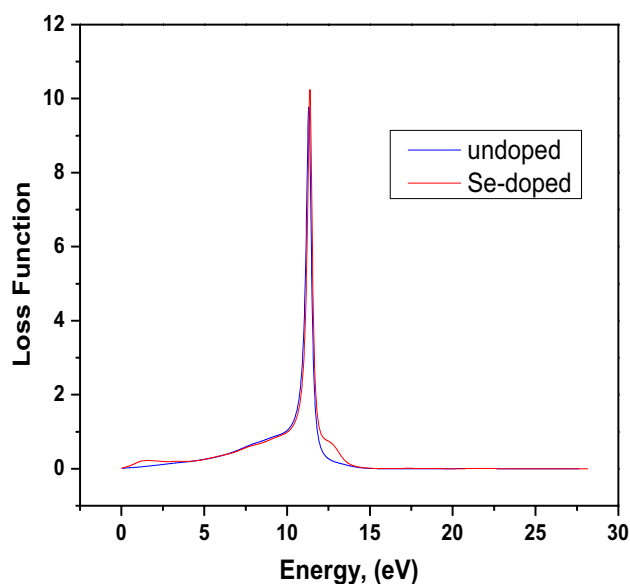


Fig. 9 Loss function for undoped and Se doped

function was found 10–12 eV for undoped crystals while two loss functions were obtained for Se doped crystals ranging 6–10 eV and small at about 35 eV.

4 Conclusion

At first, to estimate its photocatalytic activity for AgSbO_3 solid crystal molecules were investigated using first-principle calculation for their band gap, electronics properties, and optical properties. From the evidence of band structure and band gap AgSbO_3 show as better photocatalyst. The density of state for AgSbO_3 illustrates the $4d$ orbitals higher localized than $5s$ and $5p$ orbitals. The optical properties for AgSbO_3 , the optical conductivity accounts for the different of MCB and MVB which is also supporting the photocatalytic absorption of visible light for photocatalysis. The main views of this work to increase the activity using the doping technique by Se metalloids is concluded that the band gap is decreased by 0.14 eV mentioning increasing photocatalytic activities for degradation of dye or organic pollutant. As is observed of the comparative data for optical properties between undoped and Se doped crystals, there is fluctuation change with upward trends in the case of Se doped. Finally, it can be said that the photocatalytic activity was increased for Se doping with AgSbO_3 .

Acknowledgements I am thankful to my professor Dr. Parimal Bala and Dr. Kamrul Alam Khan, and Dr. Ainul Huda, Department of Physics, Jagannath University, Dhaka for their inspiration to carry on my research.

Compliance with ethical standards

Conflict of interest The authors declare that they have no competing interests.

References

1. Chen XS, Chen S, Guo L, Mao SS (2010) Semiconductor-based photocatalytic hydrogen generation. *Chem Rev* 110(11):6503–6570
2. Kumar SG, Rao KSRK (2017) Comparison of modification strategies towards enhanced charge carrier separation and photocatalytic degradation activity of metal oxide semiconductors (TiO₂, WO₃ and ZnO). *Appl Surf Sci* 391:124–148
3. Kashem MDA, Singh BR (1999) Heavy metal contamination of soil and vegetation in the vicinity of industries in Bangladesh. *Water Air Soil Pollut* 115(1–4):347–361
4. Hoque AC, Clarke A (2013) Greening of industries in Bangladesh: pollution prevention practices. *J Clean Prod* 51(2):47–56
5. Ahmed FZG, Greenleaf A, Sacks A (2014) The paradox of export growth in areas of weak governance: the case of the ready made garment sector in Bangladesh. *World Dev* 56(5):258–271
6. Hossain LS, Sarker SK, Khan MS (2018) Evaluation of present and future wastewater impacts of textile dyeing industries in Bangladesh. *Environ Dev* 26(4):23–33
7. Wang ZX, Xue M, Huang K, Liu Z (2011) Textile dyeing wastewater treatment. *Adv Treat Text Effl* 5(2):91–116
8. Cisneros RLE, Espinoza AG, Litter MI (2002) Photodegradation of an azo dye of the textile industry. *Chemosphere* 48(4):393–399
9. Wang H, Zhang L, Chen Z, Hu J, Li S, Wang Z, Liu J, Wang X (2014) Semiconductor heterojunction photocatalysts: design, construction, and photocatalytic performances. *Chem Soc Rev* 43(15):5234–5244
10. Tsuji IK, Kato H, Kobayashi H, Kudo A (2004) Photocatalytic H₂ evolution reaction from aqueous solutions over band structure-controlled (AgIn)_xZn_{2(1-x)}S₂ solid solution photocatalysts with visible-light response and their surface nanostructures. *J Am Chem Soc* 126(41):13406–13413
11. Hosogi YT, Tanabe K, Kato H, Kobayashi H, Kudo A (2003) Energy structure and photocatalytic activity of niobates and tantalates containing Sn (II) with a 5s² electron configuration. *Chem Lett* 33(1):28–29
12. Dholam RP, Patel N, Adami M, Miotello A (2009) Hydrogen production by photocatalytic water-splitting using Cr- or Fe-doped TiO₂ composite thin films photocatalyst. *Int J Hydrog Energy* 34(13):5337–5346
13. Maeda KT, Teramura K, Lu D, Takata T, Saito N, Inoue Y, Domen K (2006) Photocatalyst releasing hydrogen from water. *Nature* 440(7082):295
14. Liu WL, Liu X, Fu Y, You Q, Huang R, Liu P, Li Z (2012) Nanocrystalline pyrochlore AgSbO₃: hydrothermal synthesis, photocatalytic activity and self-stable mechanism study. *Appl Catal B* 123(3):78–83
15. Kako T, Kikugawa N, Ye J (2008) Photocatalytic activities of AgSbO₃ under visible light irradiation. *Catal Today* 131(1–4):197–202
16. Sang H-YL, Li JF (2010) Thermoelectric properties of AgSbO₃ with defect pyrochlore structure. *J Alloys Compd* 493(1–2):678–682
17. Xie WL, Li R, Xu Q (2018) Enhanced photocatalytic activity of Se-doped TiO₂ under visible light irradiation. *Sci Rep* 8(1):8752
18. Perdew JPB, Burke K, Ernzerhof M (1996) Generalized gradient approximation made simple. *Phys Rev Lett* 77(18):3865
19. Yi ZL, Liu Y, Withers RL (2010) Morphology, structure, optical, and electrical properties of AgSbO₃. *J Appl Phys* 108(2):024911

Publisher's Note Springer Nature remains neutral with regard to jurisdictional claims in published maps and institutional affiliations.